Available online at www.sciencedirect.com
SCIENCE DIRECT®
Journal of Solid State Chemistry 177 (2004) 1585–1591
JOURNAL OF SOLID STATE CHEMISTRY
http://elsevier.com/locate/jssc

Hydrothermal synthesis of nanostructured spinel lithium manganese oxide

Zhanqiang Liu,[a] Wen-lou Wang,[a,*] Xianming Liu,[b] Minchang Wu,[a] Dan Li,[a] and Zhen Zeng[a]

[a] *Department of Chemical Physics, University of Science and Technology of China, Hefei, Anhui 230026, China*
[b] *Structural Research Laboratory, University of Science and Technology of China, Hefei, Anhui 230026, China*

Received 31 July 2003; received in revised form 28 November 2003; accepted 9 December 2003

Abstract

Nanostructured spherical spinel lithium manganese oxide (LiMnO) with about 200 nm in diameter was synthesized for the first time by mild hydrothermal method. The formation of the nanostructured spheres was through self-assembly of the nanoparticles and nanobelts. The influence of the reaction temperature and the time of formation of the nanostructures have been systematically studied. The thermal stability of the nanostructures has been examined by heating-treatment at different temperatures. Powder X-ray diffraction, transmission electron microscopy, high-resolution transmission electron microscopy, thermogravimetric analysis and inductively coupled plasma-atomic emission spectroscopy were used to characterize the products.

Keywords: Nanostructure; Sphere; Spinel LiMnO; Hydrothermal synthesis; Self-assembly; Stability; Synthesis temperature and time; Calcination

1. Introduction

With the rapid development of the science and technology in laptop computer, cellular phone, digital camera and electric vehicle, the demands for high charge–discharge rate and high capacity of lithium-ion secondary batteries are increasing. Due to the low cost, high environmental acceptability and excellent voltage profile characteristics, the spinel lithium manganese oxides have been extensively studied as promising positive materials for Li-ion secondary batteries. Solid-state reaction is the conventional method to prepare spinel LiMnO after it was firstly synthesized by Wickham [1] with heating a mixture of Lithium carbonate and manganese oxide at 850°C. The products obtained by this method have a good crystallinity. But it also has several disadvantages, such as inhomogeneity, irregular morphology, large particle size, broad particle size distribution, high synthesis temperature and repeated grinding. It is well known that the particle size, the size distribution, morphology and homogeneity have important influences on the electrochemical characters of the electrode. To overcome the disadvantages of solid-state reaction, several soft chemistry methods, such as hydrothermal method [2–5], sol–gel [6–8], solvothermal method [9,10], coprecipitation [11,12] and pechini process [13] have been developed. Among these methods, solvothermal method should use organic solvents, such as alcohol, benzene as reaction mediums. It is toxic and unsafe. The sol–gel, coprecipitation and pechini process need further calcination and grinding. The hydrothermal synthesis is a powerful method to prepare various oxides. The advantage features of this method are to control the morphology, the particle size and the crystalline of products [14–18]. However, most spinel LiMnO products synthesized by the hydrothermal method reported in literature [4,5] were powders with irregular shape.

Nanostructured materials have been examined to use as cathode and anode in Li-ion battery. It has been demonstrated that nanostructured Li-ion battery electrodes show better rate capacities than conventional electrodes composed of the same materials due to the short diffusion distance of Li^+ in nanostructured electrodes [19–28]. One-dimensional nanostructured

*Corresponding author. Fax: +86-0551-363-1760.
E-mail address: wlwang@ustc.edu.cn (W.-l. Wang).

0022-4596/$ - see front matter © 2004 Elsevier Inc. All rights reserved.
doi:10.1016/j.jssc.2003.12.009

LiMnO fibers or tubes can be prepared by template method using polycarbonate filter or porous anodic aluminum oxide as templates [20,29]. This method limits the production in large scale and increases the cost of the product. Very recently, Im and Manthiram [26,27] claimed that they synthesized nanostructured spinel LiMnO by reducing lithium permanganate. The materials obtained by them showed better electrochemical performances. But lithium permanganate has a high price and is so reactive that it must be stored and handled carefully.

The cationic surfactant, such as cetyltrimethylammonium bromide (CTAB), has been extensively applied to synthesize the novel materials [30,31]. As other tetraalkylammonium salts [32], the reaction of CTA^+ cation with MnO_4^- anion can form the organic–inorganic compound ($CTAMnO_4$). This compound has been used as a manganese source to synthesize the spinel LiMnO in LiOH solution under hydrothermal condition as reported in this paper. The samples obtained were of nanostructured spherical morphology with $\sim$200 nm in diameter. The factors that affect the formation of the nanostructures, such as reaction temperature and reaction time, have been studied systematically. The thermal stability of the nanostructures was studied as well.

2. Experimental

All the chemical reagents used in the experiments were A.R. grade and used without further purification and treatment. Aqueous solutions of $KMnO_4$ (0.40 M) and CTAB (0.40 M) were mixed well by means of ultrasonication. Purple gel was rapidly formed after mixing both of these solutions. The gel was aged overnight in order to fully react between $KMnO_4$ and CTAB, and then filtrated and washed with distilled water for several times until the filtrate became colorless. The solid sample, $CTAMnO_4$, was obtained. 0.56–1.04 g $LiOH \cdot H_2O$ (depending on the reaction temperature, see Table 1) was added into the 45 mL aqueous sol–gel solution of $CTAMnO_4$ (0.40 M) and stirred for a few minutes, and then the mixed solution was transferred into a Teflon liner stainless-steel autoclave. The reactions were carried out in the temperature range from 70°C to 190°C for 4–96 h, depending on the reaction temperature (see Table 1). The samples of the reactions were filtrated, washed for several times with distilled water in order to get rid of soluble salts and then dried at 70°C in air.

Physical analysis: Powder X-ray diffraction (XRD) analysis was carried out to identify the phase of the samples using Max918AHF X-ray diffractometer (MAC Science Co. Ltd) with Cu$K\alpha$ ($\lambda = 1.54056$ Å) radiation monochromated by graphite at 40 kV and 100 mA. The morphologies of the samples were observed by transmission electron microscopy (TEM, Hitachi-H800, 200 kV) and high-resolution transmission electron microscope (HRTEM, JEOL2000, 200 kV). The samples for TEM and HRTEM were prepared by suspending powder ultrasonically in ethanol and pipetting the solution onto carbon coated copper grids. Thermogravimetric analysis (TGA) was performed in air with Shimadzu TGA-50 H thermogravimetric analyzer at a heating rate of 10°C/min.

Chemical analysis: Lithium and manganese contents of the as-prepared samples were determined by inductively coupled plasma-atomic emission spectrometer (ICP-AES, Atomscan Advantage, USA). The average valence of Mn in as-prepared and calcinated samples was measured by redox titration using $(NH_4)_2Fe(SO_4)_2$/$KMnO_4$.

Electrochemical characterization of the spinel synthesized in this paper was carried out. The spinel/carbon mixtures were thoroughly mixed with polyvinylidene fluoride (PVDF), and then composite positive material was coated on aluminum foil. The final weight ratio of spinel:carbon:PVDF was 72:20:8. The electrolyte was 1 M $LiPF_6$ in a 1:1 mixture of ethylene carbonate (EC) and dimethyl carbonate (DMC). A lithium foil was used

Table 1
Reaction conditions and properties of the synthesized spinel LiMnO[a]

Temp. (°C)	Time (h)	C_{LiOH} (M)	a_o[b] (nm)	Z_{Mn}[c]	Li/Mn	Composition[d]	r[e] (nm)
70	48	0.55	0.811	3.82	0.79	$Li_{1.32}Mn_{1.68}O_{3.88}$	7.1
90	24	0.45	0.813	3.77	0.71	$Li_{1.25}Mn_{1.75}O_{3.92}$	8.8
110	24	0.40	0.814	3.72	0.62	$Li_{1.15}Mn_{1.85}O_{4.02}$	11.2
130	24	0.30	0.815	3.67	0.51	$Li_{1.01}Mn_{1.99}O_{4.16}$	12.4
150	24	0.30	0.820	3.62	0.48	$Li_{0.97}Mn_{2.03}O_{4.16}$	15.4
170	8	0.30	0.821	3.55	0.47	$Li_{0.95}Mn_{2.05}O_{4.11}$	14.0
190	4	0.30	0.822	3.44	0.42	$Li_{0.89}Mn_{2.11}O_{4.07}$	16.3

[a] The concentration of $CTAMnO_4$ was fixed at 0.40 M.
[b] Lattice constant.
[c] Average valence of Mn.
[d] The residue of the organic materials was not added into the composition.
[e] The primary particle size calculated with Scherrer formula.

as negative electrode. Cells were cycled galvanostatically in the range from 2.75 to 4.30 V at C/2 rate for charge and discharge at room temperature.

3. Results and discussions

3.1. Effects of reaction temperature on the formation of the nanostructures

The single-phase spinel LiMnO can be obtained by hydrothermal method in a wide temperature range at appropriate concentrations of the reactants. Table 1 lists the typical reaction parameters under which the single-phase spinel LiMnO can be produced at various temperatures. The properties of the products are listed in Table 1 as well.

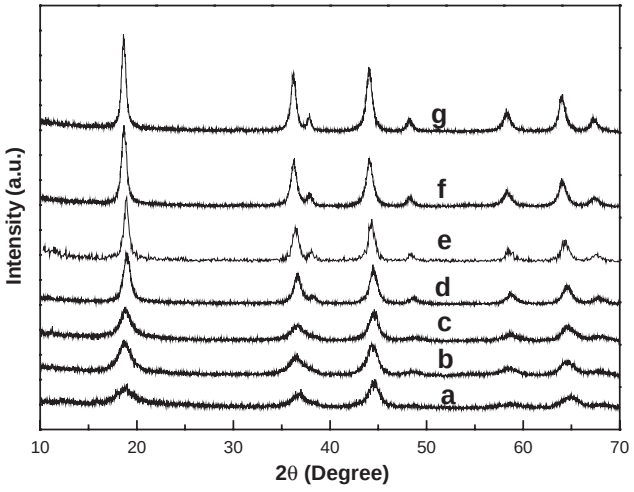

Fig. 1. XRD patterns of the products hydrothermally synthesized at: (a) 70°C; (b) 90°C; (c) 110°C; (d) 130°C; (e) 150°C; (f) 170°C and (g) 190°C.

The XRD patterns of the products listed in Table 1 are shown in Fig. 1, from which it can be seen that all diffraction peaks can be assigned to the spinel phase (JCPDS 35-782), and the peaks become sharper with the increase of the reaction temperature. This indicates that the crystallinity of the products becomes better or the primary particles grow up. The lattice constants of the samples are calculated on the basis of the XRD results using a least-squares program. Just as shown in Table 1, the lattice constants gradually increase with elevating reaction temperature from 0.811 nm at 70°C to 0.822 nm at 190°C. This behavior gets some similarity to that of the coprecipitation method reported by Chan [12]. The average valence of Mn has a reverse tendency with the temperature, indicating that the concentration of Mn^{4+} in the samples obtained at lower temperature is higher than that obtained at higher temperature, which results in the increase of the lattice constant with reaction temperature since Mn^{4+} has a smaller ionic radius than Mn^{3+}. Element analysis indicates that the Li/Mn ratios of the samples have a regular change from Li-rich at lower temperature to Li-poor at higher temperature (see Table 1).

The morphologies of the synthesized samples were observed by TEM. It is found that the nanostructured LiMnO with spherical shape can be obtained in the temperature range from 70°C to 130°C. A typical example is shown in Fig. 2. Fig 2 displays low-magnification TEM (a), high-magnification TEM (b), high-resolution TEM (c) images and ED pattern (d) of the sample synthesized at 90°C for 24 h. LMTEM image (Fig. 2a) indicates that the morphology of the sample is of spherical shape with the mean diameter of ~200 nm. Those spheres are constructed by nanoparticles and strip-like particles (Fig. 2b). HRTEM reveals that strip-like particles are nanobelts. The wideness of nanobelts is about 2 nm and the length is about a few tens nanometers (Fig. 2c). The lattice fringe is clearly seen

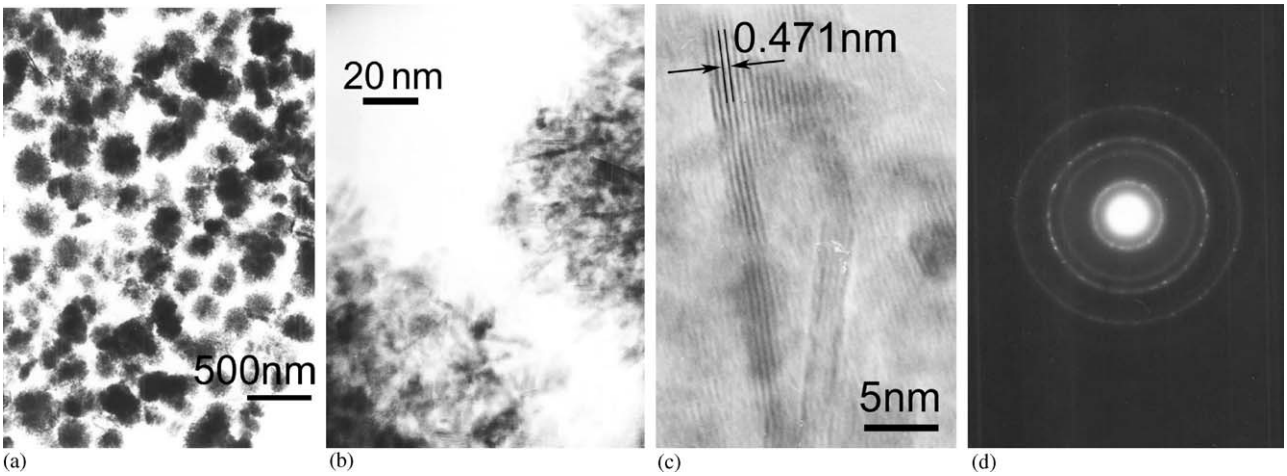

Fig. 2. TEM images (a), (b), HRTEM image (c) and SAD pattern (d) of the product hydrothermally synthesized at 90°C for 24 h.

from HRTEM image, indicating that those nanoparticles and nanobelts are crystallized. The d spacing between the lattice fringes is about 0.47 nm, which corresponds to the {111} plane of the spinel LiMnO. Fig. 2d displays the corresponding selected area diffraction pattern (SAD) of the HRTEM image. The values calculated on the basis of diffraction rings are identical with the data of XRD, indicating that the sample is of spinel structure. The diffraction rings also indicate that the primary particles are very fine, in agreement with the broad diffraction peaks shown in Fig. 1b. To the best our knowledge, this kind of nanostructured spinel LiMnO is observed for the first time. When the reaction temperature was set at 190°C, only the spinel nanoparticles with ~20 nm can be observed. In the middle temperature, such as 150°C, the sample obtained is composed of the nanostructures and nanoparticles.

The formation of the spinel may have a relation with the intermediate decomposed by $CTAMnO_4$. As other tetraalkylammonium permanganate salts [32], $CTAMnO_4$ is not stable at elevated temperature. When the temperature of the reaction system is elevated to higher than 70°C, $CTAMnO_4$ in the aqueous solution should decompose into MnO_2 colloid. The newborn MnO_2 is so chemically active that it could react easily with LiOH to give birth to the spinel LiMnO. Due to the presence of cationic surfactant, it should interact with MnO_2 colloidal particles, and therefore confines the growth of spinel LiMnO to a few nanometers as detected by XRD and TEM. The short strip-like shape of LiMnO may originate from lamellar MnO_2 (Li-Birnessite), an intermediate product that will be discussed in the next paragraph. Under the influence of surfactant, the assembly of these nanoparticles and nanostrips occurs spontaneously, as the formation of nanostructured CdS templated from cholesteryl-(ethylene oxide)$_{24}$ [33]. After the growth of the particles at higher temperature, the forces of the assembly cannot hold them together, so that the nanostructures are destroyed.

The concentrations of the reactants are crucial factors that affect the purity of the product as reported by Feng [3], Kanasaku [4] and Zhang [5]. For example, the single-phase spinel can be obtained in the concentration range of 0.30–0.40 M LiOH under 130°C conditions. Otherwise, Li_2MnO_3 or γ-MnOOH emerged in the products when the concentration of LiOH was higher or lower than the range. The spinel was precipitated together with γ-MnOOH when the LiOH concentration was 0.20 M. This impure phase disappeared with the increase of LiOH concentration (0.30–0.40 M) since γ-MnOOH is a common manganese source to synthesize spinel LiMnO [4]. Further increasing the LiOH concentration up to 1.50 M, the single-phase of Li_2MnO_3 was obtained. The similar results can be observed in other reaction temperatures. It should be pointed out that the spinel samples were precipitated together with Li-Birnessite instead of γ-MnOOH when the reaction temperature was lower than 130°C. Li-Birnessite is also a starting material to synthesize spinel LiMnO [3], so that this intermediate can be transferred to the spinel with increasing the concentration of LiOH.

3.2. Effects of reaction time on the formation of the nanostructures

In order to study the effects of reaction time on the formation of nanostructures, a series of experiments was carried out at 130°C in 0.30 M LiOH solution for 4, 12, 24, 48, 96, respectively. Figs. 3 and 4 show the XRD patterns and TEM images of as-prepared products. The XRD patterns (Fig. 3) reveal that all the products obtained at different times are the single-phase spinel LiMnO and the diffraction peaks become sharp with elongating the reaction time, indicating that the crystallinity of the products gets better or the particles grow up. TEM observation indicates that both the morphology and the particle size have apparently regular changes with the reaction time (Fig. 4). Nanostructured spherical products are formed and the primary particles are very fine when the reaction time is not too long (Figs. 4a–c). With elongating reaction time, the primary particles gradually grow up from a few nanometers to ~20 nm, which results in the collapse of the nanostructures (Fig. 4d). When the reaction time reaches 96 h, there is no trace of nanostructures but the nanoparticles with uniform size, ~20 nm (Fig. 4e). These facts indicate that the formation of nanostructured spheres is dependent on the size of the primary particles that is also dependent on the reaction time. The very fine particles formed in the short time benefit the formation of the nanostructures, whereas the larger particles destroy the nanostructures. The effect of the reaction

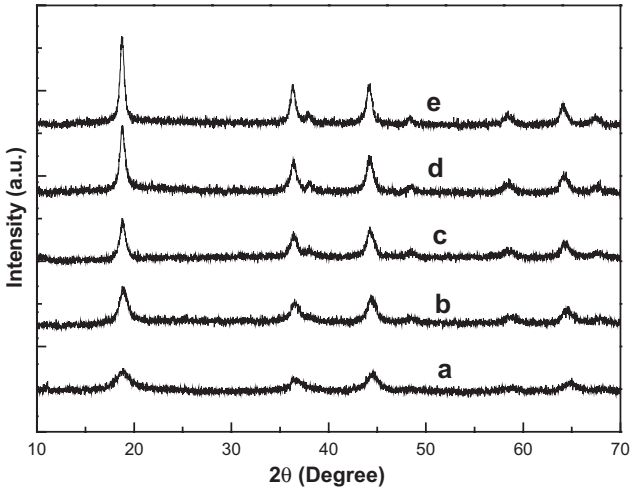

Fig. 3. XRD patterns of the products hydrothermally synthesized at 130°C at various times: (a) 4 h; (b) 12 h; (c) 24 h; (d) 48 h and (e) 96 h.

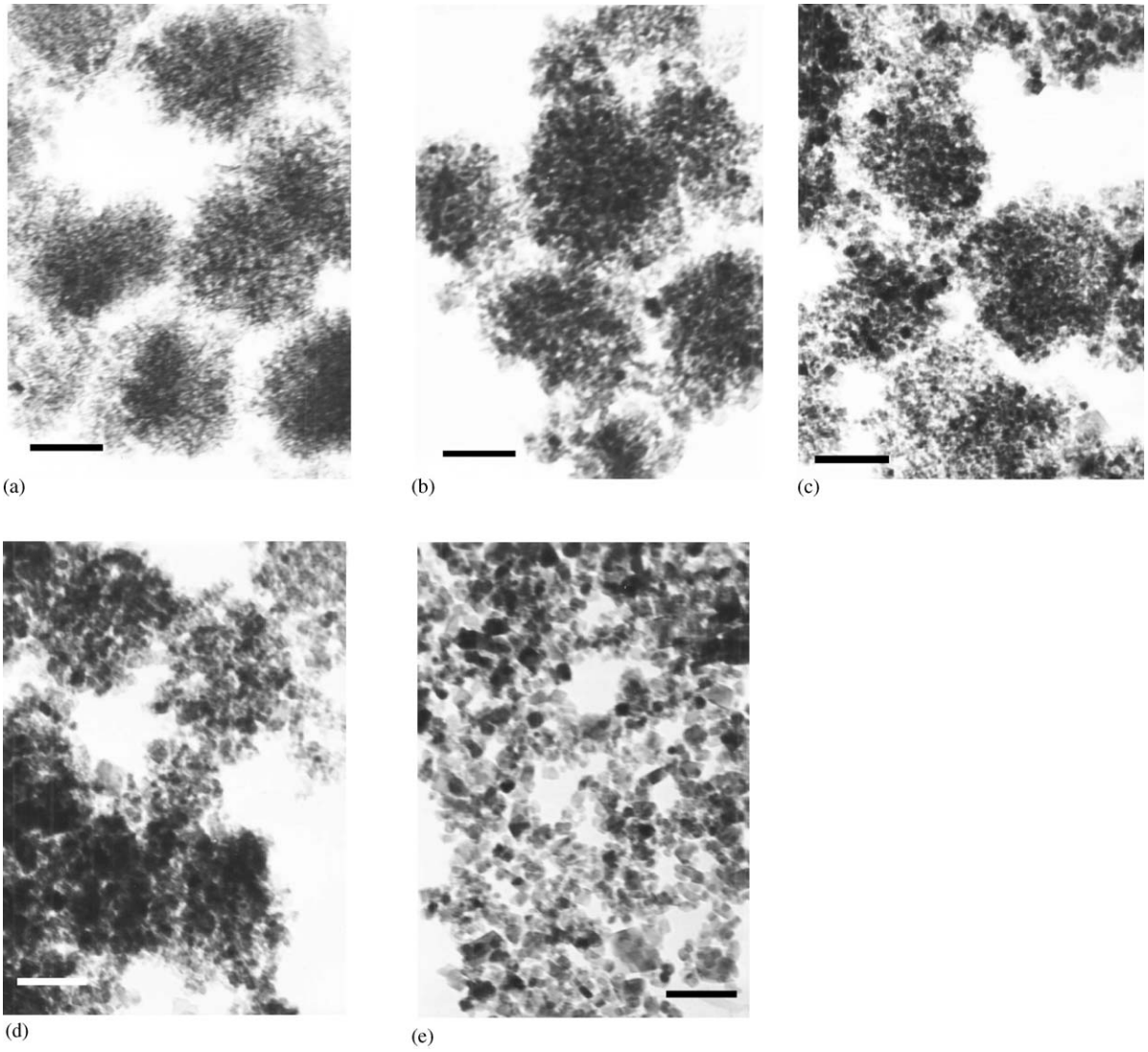

Fig. 4. TEM images of the products hydrothermally synthesized at 130°C at various times: (a) 4 h; (b) 12 h; (c) 24 h; (d) 48 h and (e) 96 h. The scale bar is 100 nm.

time is identical with the effect of the reaction temperature.

3.3. Thermal stability of the nanostructures

In order to study the thermal stability of the nanostructures, heating treatment was carried out. Fig. 5 shows the TGA curve of the sample synthesized at 90°C for 24 h (curve a). There are four discrete weight losses occurring in the regions of 30–123°C, 123–140°C, 220–330°C and 397–850°C and there is one weight increase occurring in the regions of 330–397°C. The first weight loss of 2.5% in the regions of 30–123°C is attributed to desorption of the physisorbed water in as-prepared sample. The second and the third weight loss in the regions of 123–140°C (14.30%) and 220–330°C (1.30%) mainly result from decomposition of the organic residues attached with the sample and the

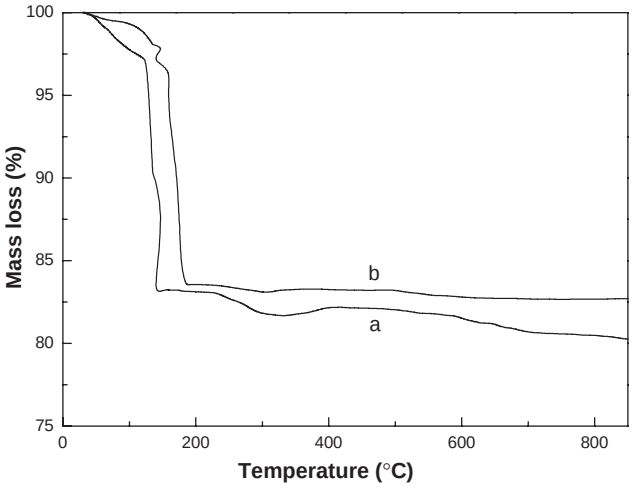

Fig. 5. TGA curves of the products synthesized at 90°C (a) and 190°C (b), respectively.

oxidation of the carbon residues left by the decomposed organic in the second region. The forth loss of 1.50% in the regions of 397–850°C should correspond to the oxygen loss [34,35]. The process of weight increase in the regions of 330–397°C may originate from the oxidization process of the sample. Curve b is the TGA result of the sample obtained at 190°C for 4 h. Generally speaking, both samples have a similar thermal behavior except the differences at reaction temperature and mass loss.

Table 2
Characters of the samples calcinated at different temperatures

Temp. (°C)	a_o [a]	Z_{Mn} [b]	Composition
300	8.17	3.63	$Li_{1.25}Mn_{1.75}O_{3.80}$
500	8.10	3.91	$Li_{1.25}Mn_{1.75}O_{4.05}$
750	8.15	3.82	$Li_{1.25}Mn_{1.75}O_{3.98}$

[a] Lattice constant.
[b] Average valence of Mn.

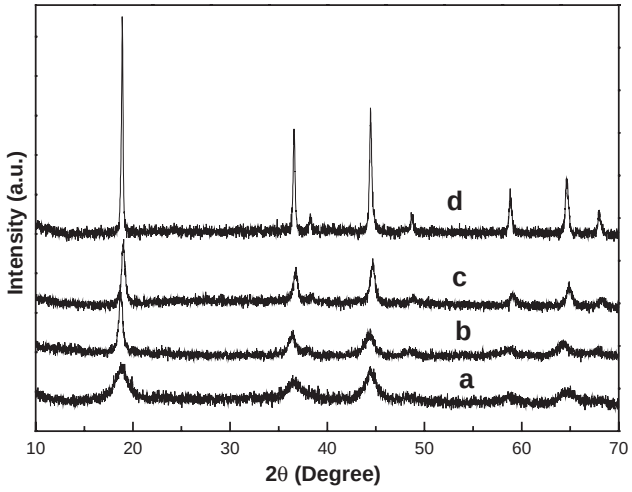

Fig. 6. XRD patterns of the product synthesized at 90°C, (a) and the samples calcinated for 5 h at: (b) 300°C; (c) 500°C and (d) 750°C.

On the basis of the TGA curve, the sample was treated by calcination at three chosen temperatures, 300°C, 500°C and 750°C for 5 h, respectively. During heating and cooling, the temperature variation was fixed at 1°C/min and the calcinated samples were characterized by XRD and TEM. The characters of the calcinated samples are listed in Table 2. The XRD patterns shown in Fig. 6 reveal that the calcinated samples are still the single-phase and the peaks become sharper than the uncalcinated sample. The lattice constant of the sample calcinated at 300°C is the largest corresponding to its lowest average valence of Mn, 3.63, which results from the reaction between manganese oxide and carbon residues in the regions of 220–330°C. The average valence of Mn decreases from RT to 300°C and increases from 300°C to 500°C, and then decreases again from 500°C to 750°C. This trend is consistent with the TGA curve just discussed above. The TEM images reveal that the nanostructured spheres can maintain up to 500°C heating treatment even though the particle sizes grow up obviously with the elevated calcination temperature (Figs. 7a–c). This phenomenon is different from that discussed in Sections 3.1 and 3.2. The post-heating treatment causes the condensation of the particles in nanostructured sphere, which can keep the nanostructures, whereas the growth of individual particle by means of elongating reaction time or increasing reaction temperature makes the larger particle come off from the nanostructures. Furthermore, the calcination at high temperature (750°C) results in the disappearance of the nanostructures and the formation of large nanoparticles with 80–150 nm in sizes (Fig. 7d). The large particles may be converted from the nanostructures through the condensation and solidification.

Preliminary electrochemical property of the sample synthesized in this work is shown in Fig. 8. The sample used as the positive electrode in cells is nanostructured

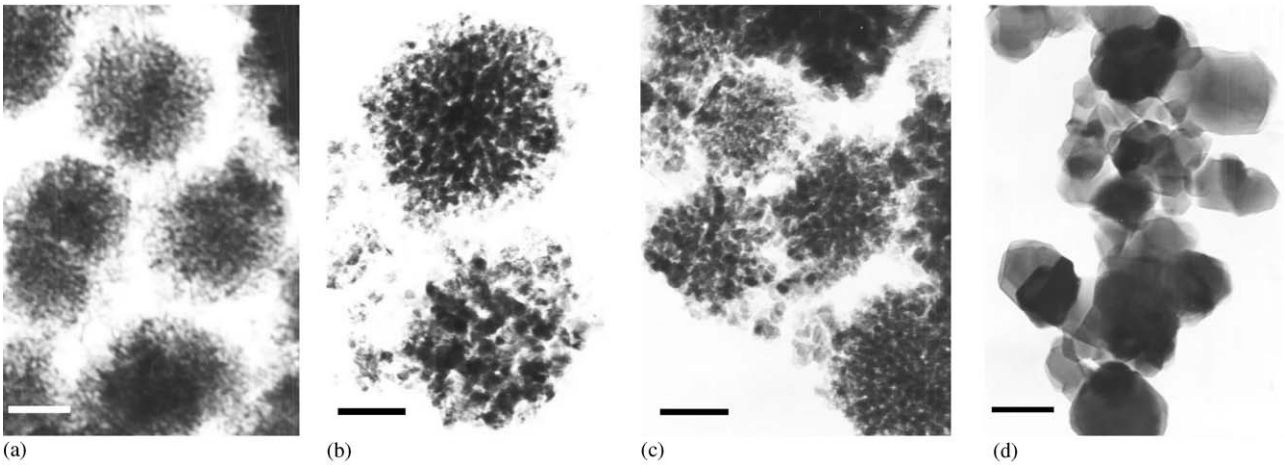

Fig. 7. TEM images of the product synthesized at 90°C, (a) and the samples calcinated for 5 h at: (b) 300°C; (c) 500°C and (d) 750°C. The scale bar is 100 nm.

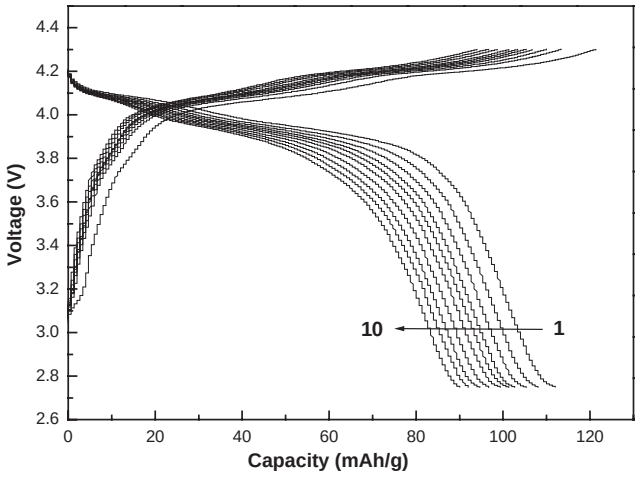

Fig. 8. Charge/discharge curves of nanostructured spinel as shown in Figs. 6b and 7b at C/2 charge/discharge rate.

spinel as shown in Figs. 6b and 7b. The preliminary result indicates that the sample is electrochemically active; however, much work should be done in order to improve electrochemical properties. The systematic study is underway; results will be reported elsewhere.

4. Conclusion

Spherical nanostructured spinel LiMnO was successfully synthesized by mild hydrothermal method. The nanostructured spinel LiMnO can be obtained at lower temperatures (70–130°C) for short reaction period. Higher reaction temperature or long reaction period result in the collapse of the nanostructures due to the primary particles growing up. The nanostructures can sustain the heating treatment up to 500°C for 5 h. At 750°C, the nanostructures convert to larger particles through condensation and solidification. Our method is suitable to produce nanostructured spinel LiMnO on large scale.

Acknowledgments

This work was financially supported by Department of Science and Technology of Anhui Province, P.R. China. Grant No. 01402003.

References

[1] D.G. Wichham, W.J. Croft, J. Phys. Chem. Sloids 7 (1958) 351.
[2] Q. Feng, H. Kanoh, Y. Miyai, K. Ooi, Chem. Mater. 7 (1995) 1226.
[3] Q. Feng, Y. Higashimoto, K. Kaijiyoshi, K. Yanagisawa, J. Mater. Sci. Lett. 20 (2001) 269.
[4] T. Kanasaku, K. Amezawa, N. Yamamoto, Solid State Ionics 133 (2000) 51.
[5] Y.C. Zhang, H. Wang, H.Y. Xu, B. Wang, et al., Solid State Ionics 158 (2003) 113.
[6] B.J. Hwang, R. Santhanam, D.G. Liu, J. Power Sources 97–98 (2001) 443.
[7] C.H. Lu, S.K. Saha, J. Sol-Gel Sci. Techn. 20 (2001) 27.
[8] R. Dziembaj, M. Molenda, D. Majda, S. Walas, Solid State Ionics 157 (2003) 81.
[9] W.J. Li, E.W. Shi, Z.Z. Chen, et al., J. Solid State Chem. 163 (2002) 132.
[10] W.L. Wang, M.C. Wu, X.M. Liu, J. Solid State Chem. 164 (2002) 5.
[11] A.R. Naghash, J.Y. Lee, J. Power Sources 85 (2000) 284.
[12] H.W. Chan, J.G. Duh, S.R. Sheen, J. Power Sources 115 (2003) 110.
[13] W. Liu, G.C. Farrignton, F. Chaput, J. Electrochem. Soc. 143 (1996) 879.
[14] X. Wang, Y.D. Li, J. Am. Chem. Soc. 124 (2002) 2880.
[15] M.H. Cao, C.W. Hu, G. Peng, et al., J. Am. Chem. Soc. 125 (2003) 1982.
[16] B. Liu, H.C. Zeng, J. Am. Chem. Soc. 125 (2003) 4430.
[17] H.C. Lee, H.J. Kim, S.H. Chung, et al., J. Am. Chem. Soc. 125 (2003) 2882.
[18] S. Wei, J. Lu, L.L. Zeng, et al., Chem. Lett. 10 (2002) 1034.
[19] C.R. Sides, N.C. Li, C.J. Martin, Patrissi, et al., MRS. Bull. 27 (2002) 604.
[20] G.L. Che, B.B. Lakshami, E.R. Fisher, C.R. Martin, Nature 393 (1998) 346.
[21] M. Nishizawa, K. Mukai, S. Kuwabata, et al., J. Electrochem. Soc. 144 (1997) 1923.
[22] N.C. Li, C.J. Patrissi, G.L. Che, C.R. Martin, J. Electrochem. Soc. 147 (2000) 2044.
[23] N.C. Li, C.R. Martin, J. Electrochem. Soc. 148 (2001) A164.
[24] N.C. Li, C.R. Martin, B. Scrosati, J. Power Sources 97–98 (2001) 240.
[25] L.F. Nazar, G. Goward, F. Leroux, et al., Inter. J. Inorg. Mater. 3 (2001) 191.
[26] D. Im, A. Manthiram, J. Electrochem. Soc. 149 (2002) A1001.
[27] D. Im, A. Manthiram, J. Electrochem. Soc. 150 (2003) A742.
[28] S. Kang, J.B. Goodenough, L.K. Rabenberg, Electrochem. Solid-State Lett. 4 (2001) A49.
[29] Y.K. Zhou, C.M. Shen, J.E. Huang, H.L. Li, Mater. Sci. Eng. B 95 (2002) 77.
[30] C.T. Kresge, M.E. Leonowicz, W.J. Roth, et al., Nature 359 (1992) 710.
[31] J.S. Beck, J.C. Vartuli, W.J. Roth, et al., J. Am. Chem. Soc. 114 (1992) 10834.
[32] S.L. Brock, M. Sanabria, S.L. Suib, J. Phys. Chem. B 103 (1999) 7416.
[33] B.M. Rabatic, M.U. Pralle, G.N. Tew, S.I. Stupp, Chem. Mater. 15 (2003) 1249.
[34] Y. Gao, J.R. Dahn, J. Electrochem. Soc. 143 (1996) 1783.
[35] Y. Gao, J.R. Dahn, J. Electrochem. Soc. 143 (1996) 100.